



**HAL**  
open science

## Interplay between silicate and hydroxide ions during geopolymerization

J. Aupoil, J.-B. Champenois, J.-B. d'Espinose de Lacaillerie, A. Poulesquen

► **To cite this version:**

J. Aupoil, J.-B. Champenois, J.-B. d'Espinose de Lacaillerie, A. Poulesquen. Interplay between silicate and hydroxide ions during geopolymerization. *Cement and Concrete Research*, 2019, 115, pp.426-432. cea-02339844

**HAL Id: cea-02339844**

**<https://cea.hal.science/cea-02339844>**

Submitted on 5 Nov 2019

**HAL** is a multi-disciplinary open access archive for the deposit and dissemination of scientific research documents, whether they are published or not. The documents may come from teaching and research institutions in France or abroad, or from public or private research centers.

L'archive ouverte pluridisciplinaire **HAL**, est destinée au dépôt et à la diffusion de documents scientifiques de niveau recherche, publiés ou non, émanant des établissements d'enseignement et de recherche français ou étrangers, des laboratoires publics ou privés.

1 Interplay between silicate and hydroxide ions during  
2 geopolymerization

3 *Julien Aupoil<sup>1,2</sup>, Jean-Baptiste Champenois<sup>1,\*</sup>, Jean-Baptiste d'Espinose de Lacaillerie<sup>2</sup>, Arnaud*  
4 *Poulesquen<sup>1</sup>*

5 <sup>1</sup>CEA, DEN, DE2D, SEAD, LCBC, F-30207 Bagnols-sur-Cèze, France

6 <sup>2</sup>Laboratoire de Sciences et Ingénierie de la Matière Molle, UMR CNRS 7615, ESPCI Paris, PSL  
7 Research University, 10, rue Vauquelin, 75231 Paris Cedex 05, France

8 \* Corresponding author

9 Keywords: silicate, hydroxide, Hammett, alkali, metakaolin, dissolution, condensation,

10

11

12 **Abstract**

13 Two set of activating solutions were prepared with increasing sodium hydroxide content, either  
14 containing or not silicates. Their alkalinities, here defined as the ability of solutions to resist  
15 changes in pH, were determined and compared by measuring Hammet acidity functions that can  
16 be assimilated to extended pH values. Such Hammet functions in sodium silicate solutions are  
17 reported for the first time. The impact of both the alkalinity and the initial Hammett function on  
18 the reactivity of metakaolin (MK)-based pastes was assessed using Isothermal Conduction micro-  
19 Calorimetry (ICC). It was concluded that the reactivity of MK mixed with sodium hydroxide  
20 solution related directly to the Hammett function values whereas in sodium silicate mixes, the  
21 alkalinity value was a more pertinent parameter. A mechanism was deduced to clarify the role of  
22 hydroxide ions during the geopolymerization, highlighting at the same time the role of silicate  
23 species as hydroxide reservoir to nurture the dissolution process.

24

## 25 **1. Introduction**

26 Geopolymers refer to alumino-silicate binders obtained by reaction of a powdered alumino-  
27 silicate source, such as dehydroxylated kaolin (metakaolin, MK), with an alkali hydroxide or  
28 alkali silicate solution, as described by Davidovits<sup>1</sup>. Schematically, the geopolymerization  
29 process can be described by three simplified steps<sup>2-5</sup>. First, MK dissolution in the activating  
30 solution provides aluminate and silicate species to the reacting medium. These species then  
31 rearrange in solution, to finally polycondense, yielding the 3D network of the hardened  
32 geopolymer.

33 Carrying out a detailed mechanistic study of these three steps is a hard task. They occur  
34 concurrently and furthermore, no realistic reaction equations can be written to describe any of  
35 these steps. However, since most of the expected reaction steps are exothermic, the use of  
36 Isothermal Conduction Calorimetry (ICC) was previously reported<sup>6-11</sup> as being an efficient tool  
37 for studying the whole geopolymerization process. Indeed, heat flow and heat profiles recorded  
38 during geopolymerization provide qualitative and quantitative information. As an example, the  
39 global geopolymerization extent at a given time has been calculated as the ratio of the cumulated  
40 heat  $Q(t)$  release to the theoretical total heat at completion,  $Q_{\max}$ <sup>6,9,10</sup>. Hence, in alkali hydroxide  
41 activating solutions free from silicates, Zhang *et al.*<sup>9</sup> reported an increase of the aforementioned  
42 geopolymerization extent with increasing hydroxide ions content.

43 The relationship between activating solution composition and geopolymerization has been the  
44 subject of an extensive body of literature. Indeed, such a topic is a key issue for the use of  
45 geopolymers and their industrial development. For examples, Rahier *et al.*<sup>12</sup> reported that the  
46 activating solution modulus, defined as the  $\text{SiO}_2/\text{Na}_2\text{O}$  molar ratio, and the amount of water,  
47 defined as the  $\text{H}_2\text{O}/\text{Na}_2\text{O}$  molar ratio, are driving parameters to tune geopolymers stoichiometry

48 and consistency respectively. At a Na/Al molar ratio equal to one, the optimal geopolymer  
49 stoichiometry can thus be reached by choosing the appropriate  $\text{SiO}_2/\text{Na}_2\text{O}$  modulus of the  
50 activating solution. Later, Duxson *et al.*<sup>13</sup> observed an increase in the proportion of unreacted  
51 metakaolin and a decrease in the geopolymers density when increasing the silicate content of  
52 activating solutions as a consequence of the resulting simultaneous increase of the  $\text{SiO}_2/\text{Al}_2\text{O}_3$   
53 and  $\text{SiO}_2/\text{Na}_2\text{O}$  molar ratios. Such a result was further rationalized by using Density Functional  
54 Theory (DFT)-based Coarse-Grain Monte-Carlo simulations<sup>14</sup>. Similarly, Zhang *et al.*<sup>10</sup> reported  
55 that an increase in the activating solution modulus, defined as the  $\text{SiO}_2/\text{Na}_2\text{O}$  molar ratio, leads to  
56 a decrease in the geopolymerization extent, evaluated by isothermal calorimetry.

57 The use of <sup>29</sup>Si Nuclear Magnetic Resonance (NMR) clearly exhibited that silicates connectivity  
58 in activating solutions increases when increasing the modulus of the solutions<sup>15-17</sup>. Duxson *et al.*<sup>13</sup>  
59 postulated that the higher the silicates connectivity, the lower the silicates species lability.  
60 According to these authors, highly connected silicate species would thus hardly rearrange and  
61 densify before gelation, leading to the formation of a gel of lesser density and thinner pore size  
62 distribution, around metakaolin grains.

63  
64 In most of the aforementioned studies, the activating solutions compositions are described in  
65 terms of silicate content,  $\text{SiO}_2/\text{Na}_2\text{O}$  and  $\text{H}_2\text{O}/\text{Na}_2\text{O}$  molar ratios. The influence of the free  
66 hydroxide ions content on the geopolymerization reaction is thus not explicit. Although it had  
67 already been mentioned by Xu and Van Deventer<sup>18</sup> and Zhang *et al.*<sup>9</sup>, to the best of our  
68 knowledge, only one scientific paper has been dedicated to that topic. Indeed, by increasing the  
69 alkali hydroxide content of activating solutions and using fly ash as an aluminosilicate source,  
70 Phair and Van Deventer<sup>19</sup> reported that a higher activating solution pH leads to a higher

71 polycondensation extent. However, pH reported values seem to be approximate as they are given  
72 only in full pH units<sup>19</sup>. In any case, these three studies<sup>9,18,19</sup> clearly highlight the importance of  
73 hydroxide ions in the geopolymerization process.

74 An effect of solution pH on aluminosilicates dissolution was indeed evidenced by Xu and Van  
75 Deventer<sup>18</sup> when studying in diluted suspensions the dissolution of 15 aluminosilicates minerals.  
76 They concluded that the extent of dissolution increases for increasing alkali hydroxide solution  
77 concentrations. Complementarily, Duxson *et al.*<sup>2</sup> (and references therein) and Granizo *et al.*<sup>20</sup>  
78 amongst others also pinpointed that the dissolution kinetics of aluminosilicate sources was highly  
79 dependent on the initial pH of the solution.

80 However, all the previously mentioned experiments<sup>2,18,20</sup> were carried out using solutions free  
81 from silicates and using high liquid to solid ratio. As such, the role of silicate species and their  
82 interplay with hydroxide ions on the dissolution step during geopolymerization have never been  
83 investigated. This literature gap may have resulted from the difficulty to assess by standard pH-  
84 metry pH values of solutions containing extremely high amounts of alkali metal ions.

85  
86 In consequence, the present study firstly aims at quantifying the hydroxide content and the  
87 alkalinity of two sets of activating solutions. Two sets of solutions of increasing sodium  
88 hydroxide content were considered: the first one with a fixed silicate content and the second one  
89 devoid of silicate species. Each time, Hammet acidity functions of studied solutions were  
90 measured instead of pH, as described in the theoretical part. The corresponding alkalinity<sup>21</sup>,  
91 defined here as the ability of a solution to resist to changes in pH, was evaluated for the two sets  
92 of solutions. Then, the geopolymers reactivity observed by mixing metakaolin into these  
93 solutions was evaluated by using Isothermal Conduction Calorimetry (ICC). Finally, these new

94 data led us to discuss the role of silicate species and their interplay with hydroxide ions during  
95 geopolymerization.

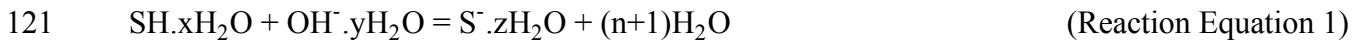
96

97 **2. Theoretical basis.**

98 In activating solutions used for geopolymers elaboration, molality of alkali metal ions can range  
99 between 1 mol / kg of water to 15 mol / kg of water. The use of a glass electrode sensitive to  
100 oxonium ions  $\text{H}_3\text{O}^+$  to assess pH values is then questionable in such media. First, a high sodium  
101 concentration in basic solutions often leads to an alkaline error, since the alkali ion concentration  
102 can be typically orders of magnitudes larger than the oxonium ions one. As an example, the alkali  
103 ion concentration is  $10^{14}$  times higher than the oxonium one in a sodium silicate solution  
104 containing 10 mol / kg of sodium ions at  $\text{pH} \approx 13$ . Then, water activity in the studied solution can  
105 be far below the value of 0.9 expected in a 3 mol / kg potassium chloride electrode filling  
106 solution. As a consequence, the ionic flow from the electrode to the studied medium could be  
107 strongly impacted, leading to false measurements. Finally, in the specific case of silicate-  
108 containing activating solutions, silicate species can interact or even deteriorate the glass electrode  
109 surface, leading to additional errors.

110 Consequently, in this work, the measurement of Hammet acidity functions<sup>22-24</sup> was chosen  
111 instead of standard pH-metry to quantify the amount of hydroxide ions in activating solutions.  
112 Such a function represents the hydroxide ions ability to deprotonate a weak acid, noted SH in  
113 reaction equation 1, added in small amounts in the aqueous medium. It is obviously equivalent to  
114 pH in dilute systems. Upon introduction in the studied medium, again in small amounts, the  
115 weak acid SH plays the role of an acid-base indicator whose ionization ratio is measured  
116 quantitatively thanks to the intensity shift of its UV-visible spectrum induced by its deprotonation  
117 . This concept was initially introduced to measure acidity of extremely acidic solution and later  
118 adapted to basic solutions, either in aqueous alkali hydroxide solutions or in non-aqueous  
119 solvents<sup>25-30</sup>.

120



122

123 In reaction equation 1, the coefficient  $n = (x + y - z)$  accounts for the difference in hydration  
124 degrees between reactants and products, according to the model used by Edward<sup>29</sup>. The  
125 corresponding equilibrium constant  $K$  is then written as:

126 
$$K = \frac{a_{\text{S}^-} \cdot a_{\text{H}_2\text{O}}^{(n+1)}}{a_{\text{SH}} \cdot a_{\text{OH}^-}} = \frac{K_a}{K_w} \quad (\text{Equation 1})$$

127 with  $a_i$  the activity of the species  $i$ .

128 As reaction equation 1 represents an acid-base reaction between the two couples SH/S<sup>-</sup> and  
129 OH<sup>-</sup>/H<sub>2</sub>O, the constant  $K$  can also be written as the ratio of the associated ionization constants:  $K_a$   
130 for the acid ionization constant of SH and  $K_w$  for the one of water (tabulated by Bandura and  
131 Lvov<sup>31</sup> and taken as  $10^{-14}$  at 25°C),

132 Hammett<sup>23</sup> defined the acidity function  $H_-$  according to equation 2. Rearranging equation 1 also  
133 provides equation 3, another definition of the acidity function:

134 
$$H_- = pK_a + \log \frac{[\text{S}^-]}{[\text{SH}]} \quad (\text{Equation 2})$$

135 
$$H_- = pK_w + \log a_{\text{OH}^-} - (n + 1) \cdot \log a_{\text{H}_2\text{O}} + \log \frac{\gamma_{\text{SH}}}{\gamma_{\text{S}^-}} \quad (\text{Equation 3})$$

136 With:

137  $pK_x$  the cologarithm of constant  $K_x$ ,

138  $\frac{[\text{S}^-]}{[\text{SH}]}$  the ionization ratio,

139  $[i]$  the concentration of species  $i$  in mol / kg of water,

140 and  $\gamma_i$  its activity coefficient defined such as  $a_i = \gamma_i \cdot [i] / [i]^\circ$  where  $[i]^\circ$  is the standard state

141 concentration of species  $i$  conventionally set equal to 1 mol / kg.

142 The experimental determination of activity coefficients being complex, equation 3 is mainly of  
143 theoretical interest, except in the rare cases when good approximations of activity coefficients<sup>24,29</sup>  
144 are possible. Nevertheless, equation 3 clearly states that the function  $H$  takes into account not  
145 only the hydroxide ions activity but also their environment through the parameter  $n$  and the  
146 variables  $a_{H_2O}$  and  $\gamma_{SH}/\gamma_{S^-}$ , respectively related to the ions hydration, the free water content and the  
147 ionic force of the solution. In consequence, the acidity function is an appropriate tool to represent  
148 the ability of hydroxide ions to react in a solution.

149 If both  $S^-$  and  $SH$  forms absorb UV-visible light at different wavelengths, the  $[S^-]/[SH]$   
150 ionization ratio can be measured by using spectrophotometry. From Beer-Lambert's law, the  
151 ionization ratio can be obtained from absorbance measurements for a constant indicator  
152 concentration according to (eq. 4).

$$153 \quad \frac{[S^-]}{[SH]} = \frac{A - A_{SH}}{A_{S^-} - A} \quad (\text{Equation 4})$$

154 With

155  $A_{SH}$  the absorbance of a solution where the indicator is fully protonated,

156  $A_{S^-}$  the absorbance of a solution where the indicator is fully deprotonated,

157  $A$  the absorbance of any basic solution with intermediate concentration.

158 A set of three solutions is thus needed to determine an ionization ratio.

159

160 **3. Experimental section.**

161 **3.1. Activating solutions elaboration**

162 Sodium hydroxide solutions were elaborated with an increasing molality ranging from  $3.17 \cdot 10^{-2}$   
 163 to  $1.40 \cdot 10^1$  mol / kg by dissolving sodium hydroxide pellets (AR grade, VWR) in ultrapure water  
 164 (18.2 MΩ). A set of alkali silicate solutions was then elaborated by diluting in water a  
 165 commercial alkali silicate solution (Betol<sup>®</sup> 52T, Wöllner: 30.2% w/w SiO<sub>2</sub>, 14.7% w/w Na<sub>2</sub>O and  
 166 55.1% w/w H<sub>2</sub>O) and by adding sodium hydroxide pellets in order to reach increasing sodium  
 167 ions molality, ranging from 5.46 to  $1.40 \cdot 10^1$  mol/kg. All solutions were stirred for at least 4 h  
 168 and cooled down to 25°C prior to any use. Solutions compositions are reported in Tables 1 and 2.

169  
 170 **Table 1.** Composition in molality, water activity and acidity function values of sodium hydroxide  
 171 solutions together with the molar ratios of the corresponding geopolymers prepared with  
 172 metakaolin. Acidity functions were taken from literature when indicated (<sup>a</sup> Rochester<sup>32</sup>,  
 173 <sup>b</sup> Schwarzenbach<sup>25</sup>).

	Solutions			Geopolymers	
	[NaOH] (mol/kg)	a <sub>H2O</sub> (± 0.008)	H.	Na/Al	$\frac{\text{SiO}_2}{\text{Na}_2\text{O}}$
<b>Na1</b>	$3.17 \cdot 10^{-2}$	1.000	12.51 ± 0.06	$3.28 \cdot 10^{-3}$	733
<b>Na2</b>	$1.00 \cdot 10^{-1}$	1.000	12.99 ± 0.06	$1.04 \cdot 10^{-2}$	232
<b>Na3</b>	$3.17 \cdot 10^{-1}$	-	13.42 ± 0.08	$3.28 \cdot 10^{-2}$	73.2
<b>Na4</b>	1.00	0.987	14.01 <sup>a</sup>	$1.04 \cdot 10^{-1}$	23.2
<b>Na5</b>	2.00	0.956	14.42 <sup>a</sup>	$2.07 \cdot 10^{-1}$	11.6
<b>Na6</b>	3.01	0.917	14.72 <sup>a</sup>	$3.11 \cdot 10^{-1}$	7.73
<b>Na7</b>	5.00	0.812	15.19 <sup>a</sup>	$5.18 \cdot 10^{-1}$	4.64
<b>Na8</b>	7.00	0.692	15.62 <sup>a</sup>	$7.25 \cdot 10^{-1}$	3.32
<b>Na9</b>	9.66	0.520	16.06 <sup>a</sup>	1.00	2.41
<b>Na10</b>	$1.20 \cdot 10^1$	-	16.47 <sup>b</sup>	1.24	1.94
<b>Na11</b>	$1.40 \cdot 10^1$	0.275	16.87 <sup>b</sup>	1.45	1.66

174  
 175  
 176

177 **Table 2.** Molality, molar ratio, water activity and acidity function values of sodium silicate  
 178 solutions. When indicated, the composition of the corresponding geopolymers prepared with  
 179 metakaolin is also given.

	Solutions						Geopolymers	
	[NaOH] <sub>added</sub> (mol/kg)	[Na] <sub>total</sub> (mol/kg)	[Si] (mol/kg)	$\frac{\text{SiO}_2}{\text{Na}_2\text{O}}$	$a_{\text{H}_2\text{O}}$ ( $\pm 0.008$ )	H.	Na/Al	$\frac{\text{SiO}_2}{\text{Na}_2\text{O}}$
<b>NaS1</b>	0	5.46	5.79	2.12	0.965	-	0.57	6.36
<b>NaS2</b>	$5.26 \cdot 10^{-1}$	6.01	5.80	1.93	0.952	$10.82 \pm 1.98$	0.62	5.79
<b>NaS3</b>	1.54	7.01	5.80	1.65	0.928	$11.64 \pm 0.35$	0.73	4.97
<b>NaS4</b>	2.54	8.02	5.79	1.45	0.903	$12.19 \pm 0.14$	0.83	4.34
<b>NaS5</b>	3.53	9.00	5.80	1.29	-	$12.52 \pm 0.10$	-	-
<b>NaS6</b>	4.20	9.68	5.80	1.20	0.837	$12.74 \pm 0.10$	1.00	3.60
<b>NaS7</b>	5.02	10.5	5.80	1.10	-	$13.10 \pm 0.11$	-	-
<b>NaS8</b>	5.52	11.0	5.80	1.05	0.767	$13.25 \pm 0.12$	1.14	3.16
<b>NaS9</b>	6.54	12.0	5.80	$9.66 \cdot 10^{-1}$	0.711	$13.59 \pm 0.20$	1.24	2.68
<b>NaS10</b>	7.54	13.0	5.79	$8.91 \cdot 10^{-1}$	0.649	$14.12 \pm 0.53$	1.34	2.32
<b>NaS11</b>	8.54	14.0	5.80	$8.27 \cdot 10^{-1}$	-	-	-	-

180

181

182

### 183 3.2. Geopolymers preparation

184 Prior to the cure and any measurements, geopolymer pastes were prepared by mixing 32.05 g of  
 185 metakaolin (MK, Metakaolin Argical M1000 from Imerys, characteristics in Table 3) with the  
 186 appropriate weight of activating solution to obtain a constant (initial water)/MK weight ratio of  
 187 0.78. Elaborated geopolymers formulations are reported in Tables 1 and 2.

188

189 **Table 3.** Physical and chemical characterization of Metakaolin by XRF, laser granulometry and  
 190 N<sub>2</sub> adsorption-desorption (with BET method) as provided by the supplier.

Oxides	SiO <sub>2</sub>	Al <sub>2</sub> O <sub>3</sub>	CaO	Fe <sub>2</sub> O <sub>3</sub>	TiO <sub>2</sub>	K <sub>2</sub> O
Composition %w/w	54.40	38.40	0.10	1.27	1.60	0.62
Granulometry (μm)	d <sub>10</sub>	1.8	d <sub>50</sub>	10.3	d <sub>90</sub>	48.2
surface area (m <sup>2</sup> /g)	18					

191

192

### 193 **3.3. Acidity function measurements**

194 Thiazole Yellow G (TYG, also known as Titan Yellow, Sigma-Aldrich) was used in the present  
195 study as the weak acid UV-visible-sensitive indicator, chosen to be compatible with the expected  
196 acidity function range of the studied solutions. Absorptions of activating solutions containing  
197 TYG were measured in the spectral range 300 to 600 nm, with a resolution of 1 nm, in 10-mm  
198 quartz cells at 25°C. Absorbance spectra were recorded on a dual-beam spectrophotometer  
199 (Genesys 10S UV-Visible, ThermoFischer Scientific), with a xenon flash lamp. Indicator-free  
200 activating solutions were used as backgrounds so that only the indicator would contribute to the  
201 recorded spectra. For the whole set of solutions, absorbance of indicator-free solutions was  
202 checked to be close to zero for wavelength ranging from 400 to 500 nm.

203 The absorbance at 480 nm has been checked to be proportional to TYG concentration up to  
204 approximately  $5 \cdot 10^{-4}$  mol / kg in sodium hydroxide solution, defining the range of validity of the  
205 Beer-Lambert law (details are available in supplementary information). Accordingly, the working  
206 concentration of TYG in all activating solutions was set to  $5 \cdot 10^{-5}$  mol / kg. In sodium hydroxide  
207 solutions, absorption bands centered at 405 and 475 nm have been observed respectively for the  
208 SH form and S<sup>-</sup> form, with an isobestic point at 433 nm. In sodium silicate solution with  
209 increasing amounts of sodium hydroxide, absorption bands were centered at 390 and 480 nm,  
210 with an isobestic point at 438 nm. Previous observations from Allain and Xue<sup>33</sup> in sodium  
211 hydroxide solutions support the existence of a simple acid-base equilibrium for TYG as described  
212 in Reaction Equation 1. Allain and Xue also reported that TYG has a good chemical resistance to  
213 hydroxide ions, and a large dynamic spectral range. In addition, the similar position of the S<sup>-</sup>  
214 form absorption band in both media corroborates the absence of any drastic conformation

215 modification, at least for the deprotonated form. This meant that silicates did not interact to any  
216 significant level with the indicator and that the latter was only involved in a simple acid-base  
217 equilibrium. Acidity functions were thus calculated from absorbance at 480 nm.

218 The  $pK_a$  of TYG has been measured in sodium hydroxide solution following Safavi and  
219 Abdollahi's procedure<sup>34</sup>. The  $pK_a$  value of  $12.92 \pm 0.01$  at  $25^\circ\text{C}$  measured in this work is  
220 consistent with the 12.92 value reported by Safavi and Abdollahi. TYG was thus considered as a  
221 suitable weak acid indicator for acidity function measurements in study alkali silicate activating  
222 solutions.

223 Finally, the working range of TYG was established (see Sup. Inf.) to be comprised between 11.9  
224 and 13.9, corresponding to an  $H$ . range equal to approximately  $pK_a \pm 1$ , which is consistent with  
225 the dynamic spectral range found by Safavi and Abdollahi<sup>34</sup> and Allain and Xue<sup>33</sup>.

226

### 227 **3.4. Water activity measurements**

228 Water activity was measured in all considered activating solutions in presence of  $5.10^{-5}$  mol/L of  
229 TYG. Measurements were done at  $25 \pm 2^\circ\text{C}$  with a Hygropalm HP23-AW-A analyzer equipped  
230 with a HC2-AW water activity probe (Rotronic) and calibrated in temperature and humidity with  
231 Rotronic certified humidity standards at 50% RH and 80% RH. After an equilibration time of  
232 5 min, water activity was measured with a precision of  $\pm 0.008$ . Water activity measurement  
233 relies on Equilibrium Relative Humidity measurement (ERH, in %), when the atmosphere in the  
234 sample holder is at equilibrium with the solution ( $a_{H_2O} = \text{ERH}/100$ ).

235

### 236 **3.5. <sup>29</sup>Si Nuclear Magnetic Resonance.**

237  $^{29}\text{Si}$  NMR measurements were performed on silicate activating solutions to investigate the silicate  
238 connectivity. Spectra were recorded at a Larmor frequency of 99.36 MHz (at  $25 \pm 2^\circ\text{C}$ ) in  
239 zirconia rotors using a Bruker Avance spectrometer and a 7-mm commercial Bruker MAS probe  
240 but without spinning. 1600 transients were acquired using a single  $90^\circ$  pulse of  $6.4 \mu\text{s}$  and a  
241 recycle time of 10 s. The recycle time was verified to be long enough by increasing it ten folds  
242 and confirming that intensities did not vary. Spectra were referenced externally to  
243 tetramethylsilane (TMS). The proportions of the different types of silicon centers were obtained  
244 by the integrated intensities of their resonances using the software Dmfit developed by D.  
245 Massiot *et al.*<sup>35</sup>. The different silicon centers were designated according to Engelhardt's  
246 nomenclature<sup>15</sup>. Each center is designated as  $Q$  since silicon atoms are quadri-coordinated to  
247 oxygen. A superscript  $Q^n$  ( $0 \leq n \leq 4$ ) indicates the number of siloxo bonds (Si-O-Si), without  
248 considering the protonation degree of non-bridging oxygens. For example  $Q^0$  designates a single  
249 silicate,  $Q^1$  a silicate with one neighbor silicate (end-chain or in a dimer) and so on. When  
250 present, subscript  $c$  indicates that silicates are part of a three-membered ring. These  $Q^2$   
251 resonances are detected at slightly different frequencies compared to the ones of  $Q^2$  groups in  
252 chains or larger rings due to their more constraint geometry.

253

### 254 **3.6. Isothermal Conduction Calorimetry**

255 Approximately 5 g of each elaborated geopolymer has been then introduced in a sealed ampoule  
256 to assess its reactivity by using Isothermal Conduction Calorimetry at  $25^\circ\text{C}$  on a TAM Air  
257 microcalorimeter. Water was used as the reference, to compensate for possible external  
258 temperature disturbances. Due to the external mixing procedure, a parasitic heat flow signal  
259 associated to the introduction of sample interfered with the initial reaction signal. The

260 equilibration time of this interference amounted to about 1.5 h, measured on an inert sample  
261 (available in supplementary information). Normalized heat flow release during  
262 geopolymerization, expressed in mW/g of paste, was recorded as a function of time during 90 h.  
263 Cumulative heat releases were obtained by integrating heat flow profiles after the end of the  
264 introduction peak here defined as when the heat flow drops to a value of 8 mW / g to minimize  
265 the contribution of the introduction peak.

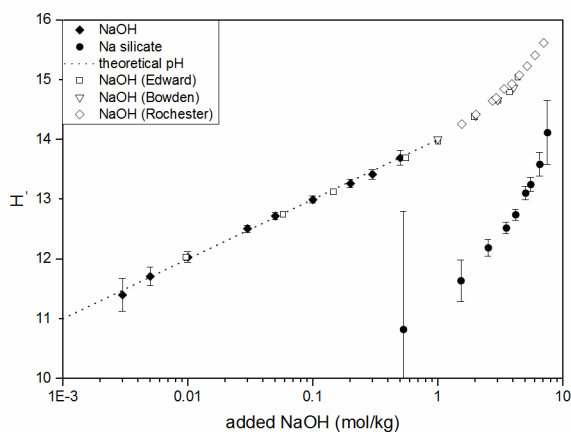
266

267

## 268 4. Results

### 269 **4.1. Acidity function $H$ and alkalinity evaluation.**

270 Acidity function values were measured for the first time in sodium silicate solutions and  
271 compared to the ones of pure sodium hydroxide solutions. Results are plotted as a function of  
272 added sodium hydroxide molality in Figure 1.



273  
274 **Figure 1.** Comparison of  $H$ . acidity function scales of pure sodium hydroxide (◆) or sodium  
275 silicate solutions (●) (with  $[Si] = 5.8 \text{ mol / kg}$ ) as a function of added sodium hydroxide  
276 molality. Literature data from Edward<sup>29</sup> (□), Bowden<sup>30</sup> (▽) and Rochester<sup>32</sup> (◇) were used for  
277 highly concentrated sodium hydroxide solutions. The dash line represents calculated theoretical  
278 pH which is equivalent to  $H$ . in dilute solutions ( $< 1 \text{ mol / kg}$ ).

279  
280 In a sodium hydroxide solution free from silicate, an addition of approximately  $0.97 \text{ mol / kg}$   
281 sodium hydroxide is needed to raise the  $H$ . value from 12.00 to 14.01 (value from Bowden<sup>30</sup>).  
282 Within this concentration range and in the specific case of pure sodium hydroxide solutions,  $H$ . is  
283 fairly equivalent to theoretical pH calculated by  $pK_w + \log [OH]$  (with a mean deviation of 0.03)  
284 and our measured values were consistent with previously reported data<sup>29</sup>. Above  $1 \text{ mol / kg}$ ,  $H$ .

285 values are out of the working range of TYG, and cannot be measured with this indicator. For  
286 sodium hydroxide addition higher than 1 mol / kg, the deviation of the  $H$ . function from the  
287 linearity is illustrated by plotting data from the literature<sup>29,30,32</sup>. Such a deviation is mainly due to  
288 a sharp decrease in water activity as mentioned by Edward<sup>29</sup>, which was measured for reference  
289 and reported in Tables 1 and 2.

290 In a silicate-containing solution, an addition of approximately 4.0 mol / kg sodium hydroxide was  
291 needed to raise the  $H$ . value from 12.19 to 13.59. For higher sodium hydroxide additions, the  
292 resulting  $H$ . function values were higher than the 13.9 threshold value of TYG working range.

293 This set of data remarkably highlights the alkalinity difference between sodium hydroxide and  
294 sodium silicate solutions. Alkalinity is here defined as the ability of a solution to resist changes in  
295 pH in a given pH range. Using this working definition, the alkalinity of both sets of studied  
296 solutions was calculated as the amount of hydroxide ions that has to be added to the solution to  
297 raise the  $H$ . value by one unit, within a  $H$ . range from 12 to 14. For  $H$ . values ranging from 12 to  
298 14, the alkalinity values were found to be 0.48 mole added hydroxide per  $H$ . unit for a silicate-  
299 free solution and 2.86 for a solution containing 5.80 mol/kg of silicate,. Within the same acidity  
300 function range, the alkalinity of the silicate-containing solution is thus more than 5 times higher  
301 than the one of the silicate-free solution.

302

## 303 **4.2. Silicate connectivity**

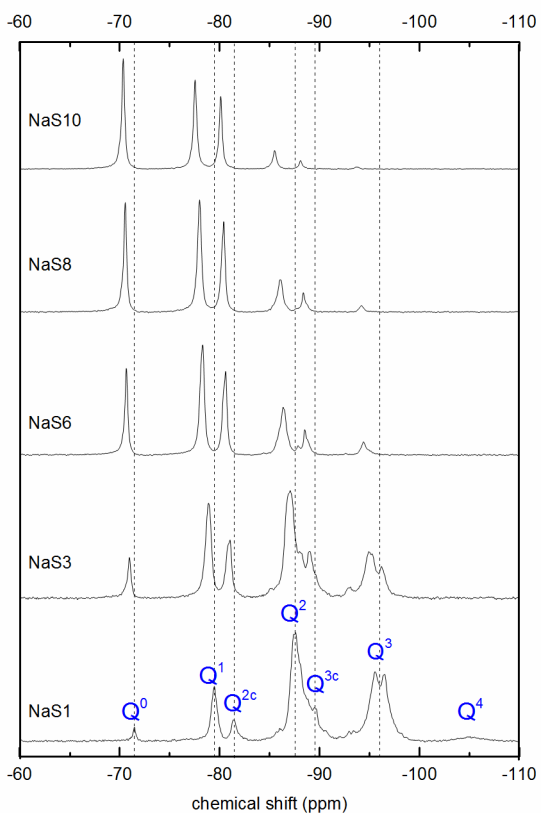
304 Liquid state <sup>29</sup>Si NMR spectra of some sodium silicate solutions investigated herein are reported  
305 on Figure 2. Several types of silicate species were present. The most deshielded are  $Q^0$  silicates ( $\delta$   
306 = -71.45 ppm in NaS1) and then  $Q^1$  ( $\delta$  = -79.45 ppm in NaS1),  $Q^2_c$  ( $\delta$  = -81.36 ppm in NaS1)  $Q^2$   
307 ( $\delta$  = -87.47 ppm in NaS1),  $Q^3_c$  ( $\delta$  = -89.55 ppm in NaS1),  $Q^3$  ( $\delta$  = -95.52 ppm in NaS1). A  $Q^4$  ( $\delta$  =

308 -105.4 ppm) resonance was only observed in NaS1. For indication, the  $^{29}\text{Si}$  resonances are known  
309 to shift to higher frequencies (higher deshielding) when increasing the alkali hydroxide content.  
310 This well-known fact is due both to the deprotonation of silanol groups (Si-OH) and to the  
311 formation of ion pairs (Si-O<sup>-</sup> +Na) according to Kinrade and Swaddle<sup>17</sup>. As expected, when the  
312 alkali hydroxide content is increased, the peak intensities decreased for highly connected silicates  
313 and increases for poorly connected silicates, reflecting the general decondensation of silica  
314 oligomers with pH. Poorly resolved  $Q^2$  and  $Q^3_c$  contributions were decomposed by fitting spectra  
315 with gausso-lorentzian lineshapes using the freeware Dmfit<sup>35</sup>. The average connectivity of Si  
316 centers was calculated from the spectral decomposition of  $^{29}\text{Si}$  NMR measurements:

$$c = \frac{\sum_n n \cdot Q^n}{\sum_n Q^n}$$

317 with  $Q^n$  the proportion of each silicate population (%).

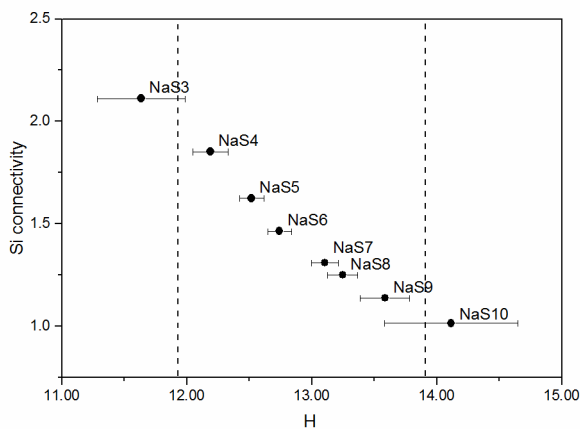
318



319  
 320 **Figure 2.** Liquid state  $^{29}\text{Si}$  NMR spectra of some sodium silicate solutions investigated herein  
 321 with varying sodium hydroxide contents. Peaks are named after Engelhardt notation<sup>15</sup>.

322  
 323 On Figure 3, the average silicate connectivity is plotted as a function of acidity function values in  
 324 silicate solutions. In the working range of TYG (dash lines), the average connectivity decreases  
 325 for increasing  $H$ . values. For sodium hydroxide additions from 2.54 to 6.54 mol/kg and  
 326 corresponding  $H$ . values ranging from 12.19 to 13.59 respectively, the silicate connectivity is  
 327 divided by almost 2. It demonstrates the decondensation of silicates species when sodium  
 328 hydroxide is added to solutions, as already reported by many authors.<sup>15-17</sup> Decondensation  
 329 consists in the hydrolysis of siloxo bonds Si-O-Si. Such an effect, highlighted by Svensson *et*

330 *al.*<sup>16</sup>, can be seen as the transfer of hydroxide ions from the solution onto silicates in the form of  
 331 Si-OH groups. This leads to the consumption of initially added hydroxide ions, as illustrated by  
 332 Reaction Equation 2:

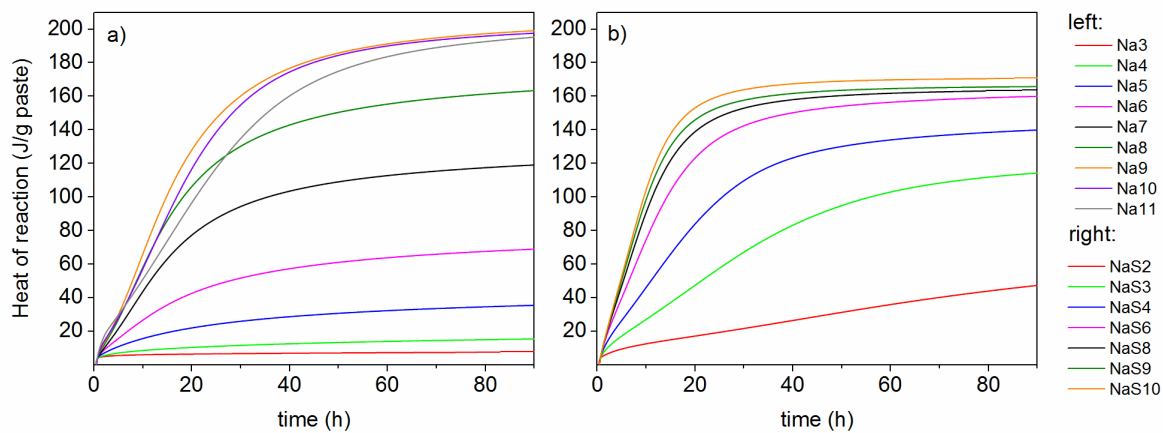


334  
 335 **Figure 3.** Evolution of the average connectivity of silicate oligomers in sodium silicate activating  
 336 solutions as a function of their acidity function *H*. along the working range of the indicator TYG.  
 337 Consequently, it was apparent that the low *H*. values in silicate solutions (<14) despite their high  
 338 sodium hydroxide contents, up to 7.5 mol/kg, were due to the presence of silicate species in  
 339 solutions and to the associated reaction described above. The presence of silicate was thus  
 340 responsible for the alkalinity measured in silicate-containing solutions.

341  
 342 **4.3. Isothermal Conduction Calorimetry measurements**

343 Metakaolin-based pastes were then prepared with the solutions under investigation. For all the  
 344 studied compositions, cumulative heat profiles could be described as a succession of two stages<sup>6-</sup>  
 345 <sup>11</sup> (Figure 4). The sharp heat release at the early beginning of the reaction can be ascribed mainly  
 346 to the metakaolin dissolution. But this contribution often overlapped second stage of the

347 geopolymerization, namely the alumino-silicate polycondensation. After a variable duration, the  
348 heat release stabilized as the reaction slowed down. The heat value at the plateau (Figure 4 and 5)  
349 could then be assumed to be approximately proportional to the extent of geopolymerization.<sup>6,9,10</sup>

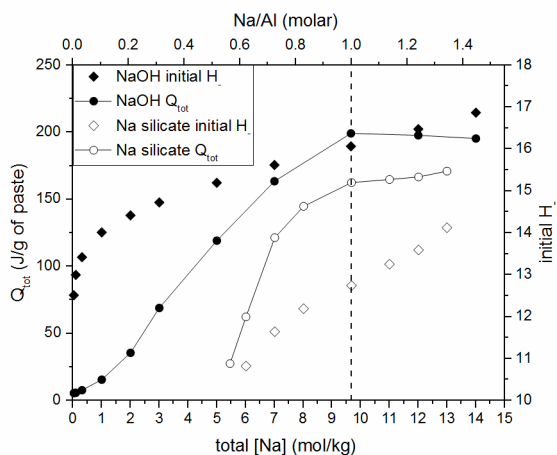


350  
351 **Figure 4.** Total heat release of geopolymer pastes prepared from a) sodium hydroxide solutions  
352 and b) sodium silicate solutions, with varying NaOH content, measured by ICC.

353

354 **5. Discussion**

355 The final heat value was plotted as a function of total sodium ions content. In the same figure, the  
356 initial  $H$ . values of the activating solutions were plotted on the right axis (Figure 5).



357

358

359 **Figure 5.** Comparison of the final heat released at 90 h of MK-based geopolymers measured by  
360 Isothermal Conduction Calorimetry (●) with the initial  $H$ . function (◆) in either pure sodium  
361 hydroxide solutions (solid symbols) or sodium silicate solutions (empty symbols) as a function of  
362 total sodium molality.

363 For both sets of experiments, i. e. with or without silicate in the activating solution, increasing the  
364 total sodium ions molality by adding sodium hydroxide up to 9.66 mol / kg led to an increase in  
365 the heat of geopolymerization. Above this 9.66 mol / kg value, the heat released during  
366 geopolymerization remained constant. It has to be noted that this molality value corresponded to  
367 a Na/Al ratio equal to 1, described in literature<sup>36</sup> as the optimal geopolymer stoichiometry due to  
368 the charge balance between  $\text{Na}^+$  ions and  $\text{AlO}_4^-$  units. At this point, the initial  $H$ . values of  
369 activating solutions amount to 12.7 and 16.1 respectively in silicate-containing and silicate-free  
370 activating solution. At this 9.66 mol / kg sodium molality, (Na/Al = 1), the  $H$ . value in the

371 silicate-containing solution was thus more than 3 units lower than in the silicate-free one. Despite  
372 this huge difference, and for the same total sodium ions concentration, geopolymerization extents  
373 were rather close in both systems.

374  
375 While, it was predictable that the composition of the reactants with respects of the stoichiometry  
376 of the final geopolymer product ( $\text{Na}/\text{Al} = 1$ ) piloted the possibility or not to reach completion,  
377 and that this explains the dependence on the sodium content of the activating solution, it  
378 remained surprising at first glance that the silicate containing activating solutions, despite their  
379 much lower initial  $H$ . values, led to large geopolymerization extent. Indeed, Xu and Van  
380 Deventer<sup>18</sup> have demonstrated among others that increasing the pH value of the dissolution media  
381 enhances alumino-silicate minerals dissolution and one might expect consequently a much lower  
382 extent of reaction for metakaolin in silicate solutions than in pure NaOH ones. The benefits in  
383 adding silicate species in activating solutions to enhance the geopolymerization process have  
384 been previously mainly attributed to their role on condensation reactions, since silicate species  
385 are available from the beginning of geopolymerization according to Duxson *et al.*<sup>13</sup>. Moreover,  
386 Phair and Van Deventer<sup>19</sup> have shown that increasing the alkali content leads to less condensed  
387 and more labile silicate species. A more porous and less dense geopolymer would thus be yielded  
388 at lower modulus  $\text{SiO}_2/\text{Na}_2\text{O}$ <sup>13,19</sup>.

389 However, the data presented here suggest another important role for the silicate species. When  
390 using a silicate-free solution as the activating solution, hydroxide ions are consumed by  
391 metakaolin dissolution, as described by Reaction Equation 3 as already reported by Xu and Van  
392 Deventer<sup>18</sup>. Due to the low alkalinity of sodium hydroxide solutions, meaning, as defined in the

393 introduction, that they do not oppose pH changes, the pH necessarily drops during reaction and,  
 394 to insure that all metakaolin is dissolved, a high initial  $H.$  value was necessary.

395



397

398 At the opposite, when a silicate-containing solution was used to activate metakaolin and for a  
 399 same Na/Al ratio (typically 1), the  $H.$  initial values were lower but a similar level of  
 400 geopolymerization was reached. Obviously, the lower acidity function  $H.$  values were  
 401 compensated by the strong alkalinity resulting from the presence of silicate species. While  
 402 hydroxide ions are also consumed by the metakaolin dissolution which releases aluminate and  
 403 silicate species in solution, following Equation 3, the hydroxide are removed from solution but  
 404 the concomitant release of silicate and aluminate species in solution favors condensation of pre-  
 405 existing alumino-silicate species, thus releasing further hydroxide ions or water molecules in  
 406 solution (Reaction Equations 4 and 5). Those freshly released hydroxide ions are then available to  
 407 react in turn at the metakaolin surface, releasing more and more silicate and aluminate species  
 408 which can feed the condensation. As a result, a chain reaction can be established thanks to this  
 409 circular mechanism that nurtures the dissolution process. This phenomenon is enhanced in  
 410 silicate-containing solutions due to their alkalinity. In other terms, the initial silicate in solution  
 411 act as a reservoir of hydroxide compensating the effect of the  $H.$  values which are initially lower  
 412 than in silicate-free solutions but remain probably somewhat constant during the dissolution.



415 It is understood, as shown in Reaction Equation 5, that condensation can also possibly release  
416 water molecules. Nevertheless, it has been shown that  $\text{Si}(\text{OH})_2\text{O}_2^{2-}$  and  $\text{Si}(\text{OH})_3\text{O}^-$  are the  
417 predominant forms of silicate monomers in activating solutions for geopolymers with respective  
418  $pK_a$ 's of 12.6 and 15.7<sup>37</sup>. Besides, silicates  $pK_a$ 's decrease with their connectivity<sup>37</sup>. In  
419 consequence, the level of silicate deprotonation should thus be significant in the present  
420 activating solutions. The release of hydroxide ions rather than water molecules would thus be  
421 favored.

## 422 **5. Conclusion**

423 Comparing initial  $H$ . values at identical Na content in sodium hydroxide and sodium silicate  
424 allowed assessing for the first time the role of activating solution alkalinity in the  
425 geopolymerization process, where the alkalinity is defined as the ability of activating solutions to  
426 resist to  $H$ . changes. As a consequence, the role of silicate species in the geopolymerization  
427 process is indirectly highlighted, since the presence of silicate species is responsible for  
428 activating solutions alkalinity.

429 The basicity of geopolymer activating solutions was investigated by UV-Visible spectroscopy  
430 using Thiazole Yellow G as a weakly acidic indicator to calculate their Hammett acidity function  
431  $H$ .. Sodium silicate and sodium hydroxide solutions alkalinity has thus been measured by using  
432 this methodology. The present results on sodium hydroxide solutions were consistent with  
433 previous results from Safavi<sup>34</sup>, validating the implemented methodology. For the first time to our  
434 knowledge, this technique was applied to alkali silicate solutions. Quantitative data on the  
435 basicity of geopolymer activating solutions were obtained, without using pH-metry. Thiazole  
436 Yellow G was an appropriate indicator to measure  $H$ . functions comprised in the range 11.9 -  
437 13.9, which is ideally suitable for concentrated alkali silicate activating solutions.

438 The variation of acidity function was found low in silicate-based solutions when compared to  
439 silicate-free solutions, for similar sodium hydroxide additions. This alkalinity difference, defined  
440 as the ability of studied solutions to resist changes in pH, is due to the condensation and  
441 decondensation of silicate species in the medium, as evidenced by using liquid state  $^{29}\text{Si}$  NMR.

442  
443 The reactivity of metakaolin-based geopolymers elaborated with previously investigated  
444 activating solutions was studied by using Isothermal Conduction Calorimetry. Taking into  
445 account initial  $H$ . values and corresponding alkalinity of activating solutions allow to precise the  
446 respective role of hydroxide ions and silicate species in the geopolymerization process. After  
447 metakaolin dissolution initiation by hydroxide ions, the “hydroxide reservoir” on silicates can  
448 gradually release hydroxide ions into the solution during the subsequent condensation of  
449 alumino-silicate species. Those freshly released hydroxide ions would then be able to dissolve at  
450 their turn additional amounts of metakaolin. This would generate a chain reaction and a self-  
451 sustained circular mechanism. This high alkalinity explain why silicate solutions of low initial  $H$ .  
452 values lead to a similar extent of geopolymerisation compared to a silicate-free solution  
453 presenting drastically higher  $H$ . values. The fact that silicate solutions allow the reaction to take  
454 place at lower hydroxide concentrations is probably crucial in directing the reaction path towards  
455 geopolymers rather than zeolites.

456 Experimental work has to be enriched to further validate this proposition, especially by  
457 measuring acidity functions during the course of geopolymerization. It must be understood  
458 however that only discontinuous measurements would be possible with this technique, after  
459 extracting the solution from the geopolymer paste at different times, since translucent media are  
460 required for absorption based methods.

461

462 **6. Conflicts of interest**

463

464 There are no conflicts to declare

## 465 7. Reference section

- 466 (1) Davidovits, J. GEOPOLYMERS - Inorganic polymeric new materials. *J. Therm. Anal.* **1991**, 37 (8), 1633-  
467 1656.
- 468 (2) Duxson, P.; Fernandez-Jimenez, A.; Provis, J. L.; Lukey, G. C.; Palomo, A.; van Deventer, J. S. J.  
469 Geopolymer technology: the current state of the art. *J. Mater. Sci.* **2007**, 42 (9), 2917-2933.
- 470 (3) Provis, J. L.; Duxson, P.; van Deventer, J. S. J.; Lukey, G. C. The role of mathematical modelling and gel  
471 chemistry in advancing geopolymer technology. *Chem. Eng. Res. Des.* **2005**, 83 (A7), 853-860.
- 472 (4) Fernandez-Jimenez, A.; Palomo, A.; Criado, M. Microstructure development of alkali-activated fly ash  
473 cement: a descriptive model. *Cem. Concr. Res.* **2005**, 35 (6), 1204-1209.
- 474 (5) Khale, D.; Chaudhary, R. Mechanism of geopolymerization and factors influencing its development: a  
475 review. *J. Mater. Sci.* **2007**, 42 (3), 729-746.
- 476 (6) Buchwald, A.; Tatarin, R.; Stephan, D. Reaction progress of alkaline-activated metakaolin-ground  
477 granulated blast furnace slag blends. *J. Mater. Sci.* **2009**, 44 (20), 5609-5617.
- 478 (7) Granizo, M. L.; Blanco, M. T. Alkaline activation of metakaolin - An isothermal conduction calorimetry  
479 study. *J. Therm. Anal. Calorim.* **1998**, 52 (3), 957-965.
- 480 (8) Yao, X.; Zhang, Z. H.; Zhu, H. J.; Chen, Y. Geopolymerization process of alkali-metakaolinite  
481 characterized by isothermal calorimetry. *Thermochim. Acta* **2009**, 493 (1-2), 49-54.
- 482 (9) Zhang, Z. H.; Wang, H.; Provis, J. L.; Bullen, F.; Reid, A.; Zhu, Y. C. Quantitative kinetic and structural  
483 analysis of geopolymers. Part 1. The activation of metakaolin with sodium hydroxide. *Thermochim. Acta*  
484 **2012**, 539, 23-33.
- 485 (10) Zhang, Z. H.; Provis, J. L.; Wang, H.; Bullen, F.; Reid, A. Quantitative kinetic and structural analysis of  
486 geopolymers. Part 2. Thermodynamics of sodium silicate activation of metakaolin. *Thermochim. Acta*  
487 **2013**, 565, 163-171.
- 488 (11) Sun, Z. Q.; Vollpracht, A. Isothermal calorimetry and in-situ XRD study of the NaOH activated fly ash,  
489 metakaolin and slag. *Cem. Concr. Res.* **2018**, 103, 110-122.
- 490 (12) Rahier, H.; Simons, W.; VanMele, B.; Biesemans, M. Low-temperature synthesized aluminosilicate  
491 glasses .3. Influence of the composition of the silicate solution on production, structure and properties. *J.*  
492 *Mater. Sci.* **1997**, 32 (9), 2237-2247.
- 493 (13) Duxson, P.; Provis, J. L.; Lukey, G. C.; Mallicoat, S. W.; Kriven, W. M.; van Deventer, J. S. J.  
494 Understanding the relationship between geopolymer composition, microstructure and mechanical  
495 properties. *Colloid Surf. A-Physicochem. Eng. Asp.* **2005**, 269 (1-3), 47-58.
- 496 (14) White, C. E.; Provis, J. L.; Proffen, T.; van Deventer, J. S. J. Molecular mechanisms responsible for the  
497 structural changes occurring during geopolymerization: Multiscale simulation. *Aiche J.* **2012**, 58 (7),  
498 2241-2253.
- 499 (15) Engelhardt, G.; Zeigan, D.; Jancke, H.; Hoebbel, D.; Wieker, W. <sup>29</sup>Si NMR-Spectroscopy of Silicate  
500 Solutions .II. Dependence of Structure of Silicate Anions in Water Solutions from Na:Si Ratio. *Z. Anorg.*  
501 *Allg. Chem.* **1975**, 418 (1), 17-28.
- 502 (16) Svensson, I. L.; Sjoberg, S.; Ohman, L. O. Polysilicate Equilibria in Concentrated Sodium Silicate  
503 Solutions. *J. Chem. Soc., Faraday Trans. 1* **1986**, 82, 3635-3646.
- 504 (17) Kinrade, S. D.; Swaddle, T. W. Silicon-29 NMR Studies of Aqueous Silicate Solutions .1. Chemical  
505 Shifts and Equilibria. *Inorg. Chem.* **1988**, 27 (23), 4253-4259.
- 506 (18) Xu, H.; Van Deventer, J. S. J. The geopolymerisation of alumino-silicate minerals. *Int. J. Miner.*  
507 *Process.* **2000**, 59 (3), 247-266.
- 508 (19) Phair, J. W.; Van Deventer, J. S. J. Effect of the silicate activator pH on the microstructural  
509 characteristics of waste-based geopolymers. *Int. J. Miner. Process.* **2002**, 66 (1-4), 121-143.

- 510 (20) Granizo, N.; Palomo, A.; Fernandez-Jimenez, A. Effect of temperature and alkaline concentration on  
511 metakaolin leaching kinetics. *Ceram. Int.* **2014**, *40* (7), 8975-8985.
- 512 (21) Drever, J. I. *The Geochemistry of Natural Water*. Pearson Education Canada: 1988.
- 513 (22) Flexser, L. A.; Hammett, L. P.; Dingwall, A. The Determination of Ionization by Ultraviolet  
514 Spectrophotometry: Its Validity and its Application to the Measurement of the Strength of Very Weak  
515 Bases. *J. Am. Chem. Soc.* **1935**, *57* (11), 2103-2115.
- 516 (23) Hammett, L. P.; Deyrup, A. J. A SERIES OF SIMPLE BASIC INDICATORS. I. THE ACIDITY FUNCTIONS OF  
517 MIXTURES OF SULFURIC AND PERCHLORIC ACIDS WITH WATER. *J. Am. Chem. Soc.* **1932**, *54* (7), 2721-  
518 2739.
- 519 (24) Hammett, L. P. THE THEORY OF ACIDITY. *J. Am. Chem. Soc.* **1928**, *50* (10), 2666-2673.
- 520 (25) Schwarzenbach, G.; Sulzberger, R. Über die Alkalinität starker Lösungen der Alkalihydroxyde. *Helv.*  
521 *Chim. Acta* **1944**, *27* (1), 348-362.
- 522 (26) Paul, M. A.; Long, F. A. H<sub>0</sub> AND RELATED INDICATOR ACIDITY FUNCTIONS. *Chem. Rev.* **1957**, *57* (1),  
523 1-45.
- 524 (27) Stewart, R.; Odonnell, J. P. STRONGLY BASIC SYSTEMS .III. H. FUNCTION FOR VARIOUS SOLVENT  
525 SYSTEMS. *Can. J. Chem.-Rev. Can. Chim.* **1964**, *42* (7), 1681-1693.
- 526 (28) Rochester, C. H. Correlation of Acidity Functions with Equilibria of p-Nitroaniline in Aqueous Sodium  
527 Hydroxide Solution. *Trans. Faraday Soc.* **1963**, *59* (492), 2820-2825.
- 528 (29) Edward, J. T.; Wang, I. C. IONIZATION OF ORGANIC COMPOUNDS .II. THIOACETAMIDE IN AQUEOUS  
529 SODIUM HYDROXIDE. THE H. ACIDITY FUNCTION. *Can. J. Chem.-Rev. Can. Chim.* **1962**, *40* (3), 399-407.
- 530 (30) Bowden, K. ACIDITY FUNCTIONS FOR STRONGLY BASIC SOLUTIONS. *Chem. Rev.* **1966**, *66* (2), 119-  
531 131.
- 532 (31) Bandura, A. V.; Lvov, S. N. The ionization constant of water over wide ranges of temperature and  
533 density. *J. Phys. Chem. Ref. Data* **2006**, *35* (1), 15-30.
- 534 (32) Rochester, C. H. Correlation of Reaction Rates with Acidity Functions in Strongly Basic Media .Part 2.  
535 Reaction of 2,4-Dinitroaniline With Aqueous Sodium Hydroxide. *Trans. Faraday Soc.* **1963**, *59* (492),  
536 2826-2837.
- 537 (33) Allain, L. R.; Xue, Z. L. Optical sensors for the determination of concentrated hydroxide. *Anal. Chem.*  
538 **2000**, *72* (5), 1078-1083.
- 539 (34) Safavi, A.; Abdollahi, H. Optical sensor for high pH values. *Anal. Chim. Acta* **1998**, *367* (1-3), 167-173.
- 540 (35) Massiot, D.; Fayon, F.; Capron, M.; King, I.; Calvé, S. L.; Alonso, B.; Durand, J. O.; Bujoli, B.; Gan, Z.;  
541 Hoatson, G. Modelling one- and two-dimensional solid-state NMR spectra. *Magn. Reson. Chem.* **2002**, *40*  
542 (1), 70-76.
- 543 (36) Rahier, H.; VanMele, B.; Biesemans, M.; Wastiels, J.; Wu, X. Low-temperature synthesized  
544 aluminosilicate glasses .1. Low-temperature reaction stoichiometry and structure of a model compound.  
545 *J. Mater. Sci.* **1996**, *31* (1), 71-79.
- 546 (37) Sefcik, J.; McCormick, A. V. Thermochemistry of aqueous silicate solution precursors to ceramics.  
547 *Aiche J.* **1997**, *43* (11), 2773-2784.

548